

Some Optical Properties of A Non-Equidiameter Electrostatic Lens Using an Integral Method

¹Tahani A. Salman and ²Basma Hussien

¹School of Applied Sciences, University of Technology, Baghdad, Iraq

²School of Applied Sciences, Al-Nahrain University, Baghdad, Iraq

Abstract: A computational investigation has been carried out in the field of non-relativistic charged-particle optics using the charge density method as a boundary value problem with the aid of a personal computer under the absence of space-charge effects. This research has been concentrated on designing a non-equidiameter electrostatic immersion lens whose electrodes are cylindrical in shape separated by an air gap. The variable parameter of the 2 electrodes is the applied voltage ratio. The axial potential distribution of an electrostatic immersion lens has been computed by taking into consideration the distribution of the charge density due to the voltages applied on the 2 cylindrical electrodes. Potentials have been determined anywhere in space by using Coulomb's law. The optical properties of the immersion lens have been investigated under finite and zero magnification conditions.

Key words: Optical properties, non-equidiameter, integral method, particle optics

INTRODUCTION

The charge density method for solving Laplace's equation was first applied in electron-optical systems by Cruise and Cruise (1963). He computed the potential distribution in an axially symmetric electrostatic lens, which contained no insulators. This method is based on a simple fact that in the static case any region occupied by a conductor is free of field. If potentials are applied on the conductors (e.g., electrodes) the charges distribute themselves on the surfaces which become equipotentials. This is equivalent to forcing definite charge distribution on the electrode (Renau *et al.*, 1982). These charge distributions are considered to be the sources of the electrostatic potential distribution in the space surrounding the electrodes including the electrode potentials themselves. If the electrode potential can be replaced by these surface charge distributions on the electrodes, the value of the potential may be easily calculated anywhere in the space by simply using the superposition principle without employing any sophisticated computational grids as in the finite-difference or finite-element methods (Harting and Read, 1976; Mautz and Harrington, 1972; Van Hoof, 1980).

This method has been found to give accurate results, efficient in the use of computer time and storage and applicable to a wide range of lens configurations. The charge density method is a particular example of Boundary Element Method (BEM). In most of the published

research the lenses that are used for this purpose have been divided into N-rings; these rings are of variable width and are made narrower near the gap, where the charge density changes most rapidly (Mautz and Harrington, 1972; Fung, 1998). However, in the present research the system of cylinders under applied potential has been replaced by a system of charged rings, which have the same width as illustrated in Fig. 1.

Three of the various magnification conditions that are well known in electron optics have been taken into account in the present research, namely, the infinite, finite and the zero magnification conditions due to their resemblance to the trajectory of charged particles traversing a lens field. Because of the complex nature of the present problem under investigation, the following assumptions have been made the thickness of the material

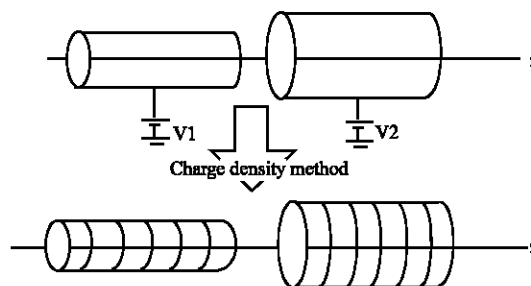


Fig. 1: Replacing a series of cylinders under applied potentials with a series of charged rings (6)

from which the lenses should be constructed is negligible compared to the radii of the cylinders. The space charge effects are neglected in order to satisfy exactly the Laplace's equation $\nabla^2\phi = 0$ and Non-relativistic velocities for the accelerated charged particles have been taken into consideration.

MATERIALS AND METHODS

The 1st step in the present method for calculating the axial potential distribution of a 2-cylinder electrostatic lens is to find the charge density on each surface of the conducting sheets from which the lens is constructed. In the absence of dielectrics the electrostatic potential at any point in space is determined by the free surface charges on the conductors in the space (Read *et al.*, 1971).

The 2nd step is, therefore, to use the determined charge density for computing the potential distribution in the space of the lens. In applying this method for non-equidiameter coaxial cylinders separated by a finite distance G , it has been assumed that the cylinder walls have negligible thickness so that the potential in regions which are not very close to the cylinders is determined simply by the algebraic sum of the inner and outer charge sheets (Bonjour, 1980). To solve the problem, the cylinders have been divided into N rings; each ring carries a charge Q_i ($i = 1, 2, 3, \dots, N$), which contributes to the potentials of all the rings (Fig. 2). The potential of the i th ring can be expressed as a combination of the contributions from all charged rings (Fung, 1998). Consider the lens cylinders shown in Fig. 2 of radii r_1 for the 1st electrode, r_2 for the second electrode and length $20r_2$ (Mulvey and Wallington, 1973). The combined charge densities on the surfaces of the cylinders are:

$$\sigma_i = Q_i / \pi (r_1 + r_2) \Delta z_i$$

where:

Δz_i = The width of i th ring

If there are no other charges present then the potential at any point z in space is given by,

$$U(r_1 r_2, z) = \frac{1}{\pi \epsilon_0} \sum_{i=1}^N \sigma_i k_i K(k_i^2) \Delta z_i \quad (1)$$

Where:

$$k_i = \frac{r_1 + r_2}{\left[(r_1 + r_2)^2 + (z_i - z)^2 \right]^{1/2}}$$

and $K(k^2)$ is the complete elliptic integral of the first kind, which can be evaluated by the use of the following polynomial approximation (Szilagy, 1988),

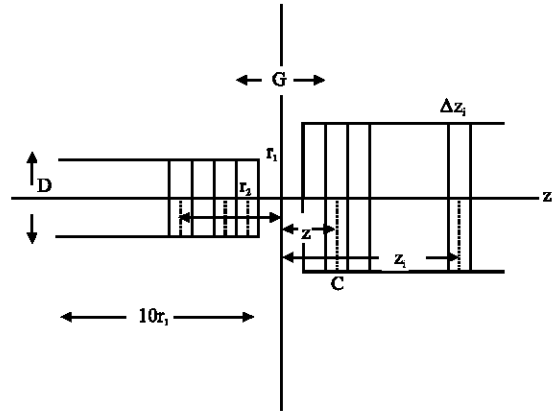


Fig. 2: Simple coaxial 2-cylinder lens consisting of a large number of circular strips in order to obtain the potential distribution by CDM

$$K(k_i) = a_0 + a_1 H + a_2 H^2 + a_3 H^3 + a_4 H^4 + (b_0 + b_1 H + b_2 H^2 + b_3 H^3 + b_4 H^4) \ln(1/H) \quad (2)$$

where, $H = 1 - k_i^2$, which is a dimensionless factor.

The potential V_j at a point C in Fig. 2 on the i th element is due to a constant charge density σ on each element, which is uniformly distributed around a circle of radii r_1, r_2 . The potential V_j is given by the following expression (Harting and Read, 1976),

$$V_j = \sum_{i=1}^N A_{ji} \sigma_i \quad (3)$$

where:

A_{ji} = A square matrix element

The above set of Eq. 3 may be reduced to the following simple matrix equation:

$$V = A \cdot \sigma \quad (4)$$

The charge density σ is mathematically considered a column vector. In applying this procedure to the cylinder problem one may take different values of the voltage applied on the 1st and 2nd electrodes, the column vector σ is then obtained by inverting the matrix (Renau *et al.*, 1982; Mautz and Harrington, 1972). Hence, from Eq. 4,

$$\sigma = A^{-1} \cdot V \quad (5)$$

In the present research, an iterative procedure is used to get the inverse of matrix A with the aid of a computer program based on LU-Factorization method (Kolman, 1985). To evaluate the elements of A one needs to know

the potential at the strip j caused by a uniform charge density σ_i in the strip i. The matrix element A_{ji} is given by (Mulvey and Wallington, 1973),

$$A_{ji} = \frac{k_{ji} \Delta z_i}{\pi \epsilon_0} K(k_{ji}^2) \quad (6)$$

Where:

$$k_{ji} = \frac{r_1 + r_2}{\left[(r_1 + r_2)^2 + (z_1 - z_2)^2 \right]^{1/2}}$$

and

$$z_{ji} = \left| \bar{z}_i - \bar{z}_j \right|$$

\bar{z}_i and \bar{z}_j being the mid point of the ith and jth ring respectively; they are given by $\bar{z}_i = (z_{i+1} + z_{i-1})/2$ and $\bar{z}_j = (z_{j+1} + z_{j-1})/2$. It should be noted that when j is equal to i the elliptic integral (Eq. 2) will be infinite and a singularity in the potential V is caused but not in A_{ji} itself.

THE TRAJECTORY EQUATION AND LENS ABERRATION

The equations of motion of a charged particle traveling at a non-relativistic velocity in an electric field near the axis of a cylindrically symmetric system can be reduced to the following paraxial ray Eq. 7 (Grivet, 1972; Paszkowski, 1968),

$$\frac{d^2 R}{dz^2} + \frac{U'}{2U} \frac{dR}{dz} + \frac{U''}{4U} R = 0 \quad (7)$$

where, U' and U'' are the 1st and 2nd derivatives of the axial potential U, respectively. R represents the radial displacement of the beam from the optical axis z and the primes denote a derivative with respect to z.

The most important aberrations in an electron-optical system are spherical and chromatic aberration. Thus the present research has been focused on determining these 2 aberrations for an immersion electrostatic lens operated as an objective lens. The spherical and chromatic aberration coefficients are denoted by Cs and Cc, respectively. In the present investigation the values of Cs and Cc are normalized in terms of the image side focal length, i.e., the relative values of Cs/f_i and Cc/f_i are investigated as figures of merit, which are dimensionless.

The spherical aberration coefficient Cs and the chromatic aberration coefficient Cc referred to the image/object side are calculated from the Eq. 8 (Szilagy, 1988).

$$C_s = \frac{U^{-1/2}}{16R'^4} \int_{z_0}^{z_i} \left[\frac{5}{4} \left(\frac{U''}{U} \right)^2 + \frac{5}{24} \left(\frac{U'}{U} \right)^4 + \frac{14}{3} \left(\frac{U'}{U} \right)^3 \frac{R'}{R} - \frac{3}{2} \left(\frac{U''}{U} \right)^2 \frac{R'^2}{R} \right] \sqrt{U} R^4 dz \quad (8)$$

$$C_c = \frac{U^{1/2}}{R'^2} \int_{z_0}^{z_i} \left(\frac{U'}{2U} R'R + \frac{U''}{4U} R' \right) U^{-1/2} dz \quad (9)$$

where, U = U(z) is the axial potential, the primes denote derivative with respect to z and $U_i = U(z_i)$ is the potential at the image where $z = z_i$. The integration given in the Eq. 8 and 9 are executed by means of Simpson's rule (Szilagy, 1988; Hawkes, 1980). In the present research, Eq. 8 and 9 have been used for computing Cs and Cc in the image side under various magnification conditions.

RESULTS AND DISCUSSION

The charge density and the corresponding potential distributions at various values of the optical considerably along the surface of each electrode as shown in Fig. 3 and 4 under accelerating mode of operation. The air gap between the 2 non-equidiameter cylindrical electrodes is defined in Fig. 1. The voltages applied on the electrodes are $V_1 = 10V$ and $V_2 = 18V$. Due to the limited number of elements of the matrix A each electrode has been divided into ten equal rings. The charge density distribution due to the varies applied voltages on the electrodes region each point on the graph represents a uniform charge density for a particular ring. The voltage applied on the electrode positioned at the right-hand side of the air gap greater than that on the left-hand side. Within the air gap there is no charge density due to the rings situated at the two terminals of each cylinder, which are at a close proximity to air. Furthermore, the ratio of the charge density on the terminal ring at the lower voltage found to be equal to 1.8, which is the ratio of the voltages applied on the 2 electrode. It must be made clear that even at higher applied voltages the above mentioned charge density ratio still equals to the applied voltage ratio.

The axial potential distributions at various values of the optical axis are shown in Fig. 4. This is a field-free region when $E(Z) = 0$ outside the lens boundaries. These potentials are similar in their general form. The potential U(Z) at point (Z = 0.0) equals to 15.5 V, this value does not represent the average of the potentials applied on the 2 electrodes because the field shifted to the electrode, which has a radius less than the radius of the 2nd electrode.

The electron beam path along the electrostatic lens field under zero magnification condition and accelerating

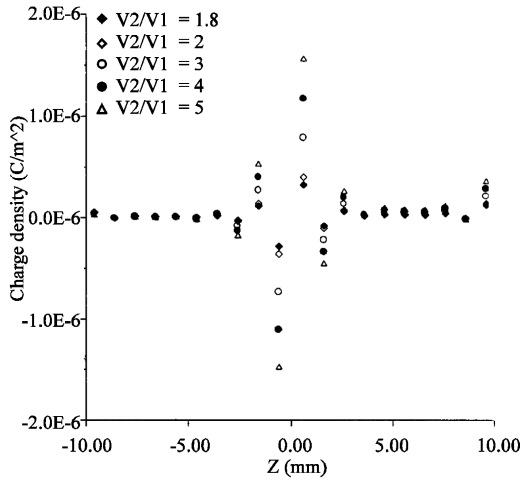


Fig. 3: The charge density distribution on 2 electrodes at different values of the voltage ratio ($V_2/V_1=1.8, 2-5$)

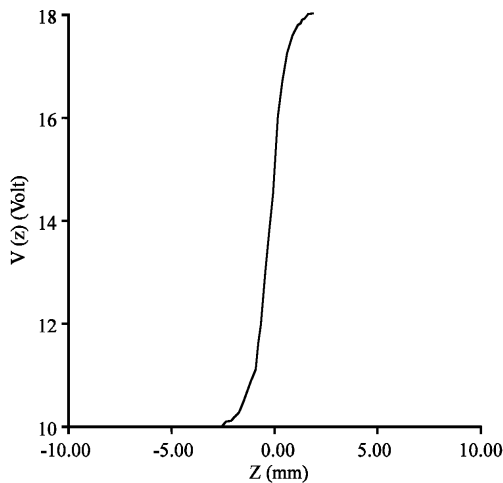


Fig. 4: The axial potential distribution on the 2 electrodes (r_1, r_2) under accelerating mode of operation

mode of operation has been considered. Figure 5 shows the trajectories of an electron beam traversing the electrostatic lens field at various values of both voltage ratios V_2/V_1 . These trajectories have been computed with the aid of Eq. 7 taking in to account that the total length of the 2 electrodes ($L = 20$ mm) the air gap ($G = 1$ mm) and the radius ($r_1=0.5$ mm) and radius ($r_2 = 1$ mm) the 2 non-equidiameter cylindrical electrode are kept constant. Computation have shown that as the beam emerges from the lens field it converges towards the optical axis provided this is due to the increase of the voltage ratio. The trajectories are generally similar in their form.

The electron beam path along the electrostatic lens field under finite magnification condition and accelerating mode of operating has been considered. Figure 6 shows

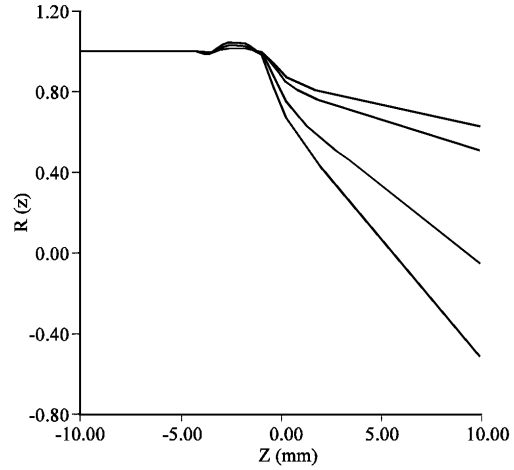


Fig. 5: The electron beam trajectory in an electrostatic lens under zero magnification condition at various values of the voltage ratio ($V_2/V_1=1.8, 2-5$)

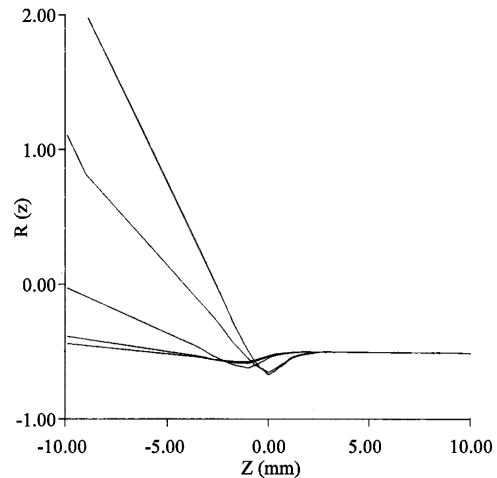


Fig. 6: The electron beam trajectory in an electrostatic lens under finite magnification condition at various values of the voltage ratio ($V_2/V_1=1.8, 2-5$)

the trajectories of an electron beam traversing the electrostatic lens field at various values of both voltage ratios V_2/V_1 . These trajectories have been computed with the aid of Eq. 7. The value of the trajectory slope at object position highly affects the magnification. These trajectories are similar in their general form. Further more, the radial displacement of the beam increase with increasing voltage ratio at values of ($V_2/V_1=1.8, 2, 3, 4, 5$) trajectories have across over within the air gap region.

Figure 7 shows the trajectories of an electron beam transverse the electrostatic lens field at various values of V_2/V_1 . These trajectories have been computed with the aid of Eq. 2-7. It is seen that as the voltage ratio V_2/V_1 increase the $R(z)$ is decreases.

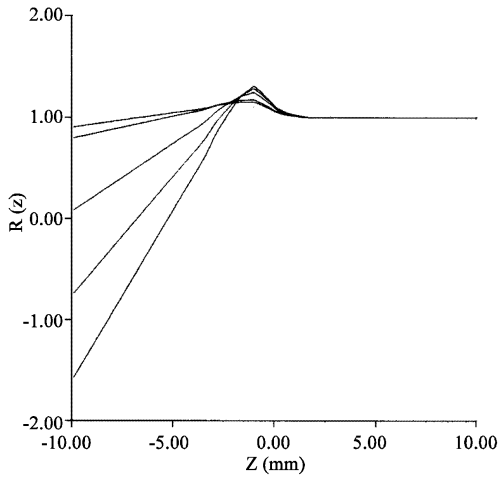


Fig. 7: The electron beam trajectory in an electrostatic lens under infinite magnification condition at various values of the voltage ratio ($V_2/V_1 = 1.8, 2-5$)

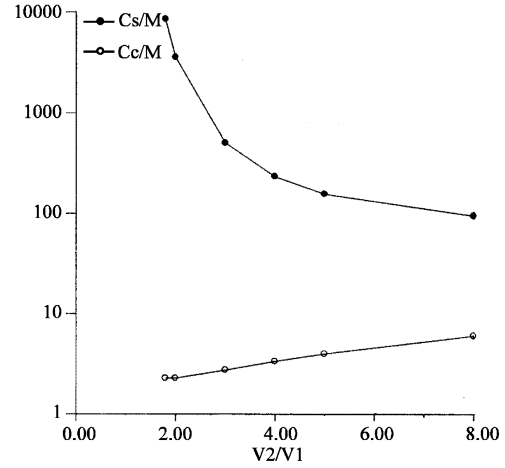


Fig. 9: The spherical and chromatic aberration coefficient under finite magnification condition

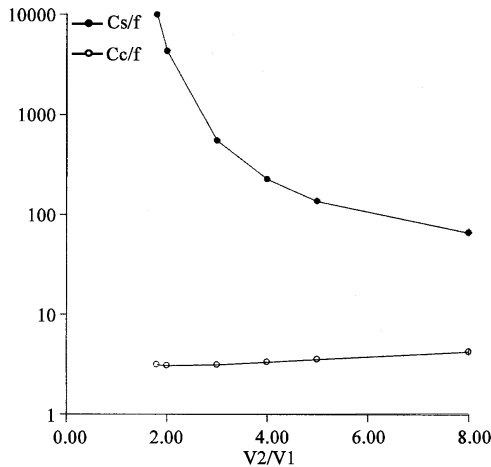


Fig. 8: The spherical and chromatic aberration coefficients under zero magnification condition

The spherical and chromatic aberration coefficients have been given considerable attention in the present research, since they are the 2 most important aberrations in electron optical system.

Under zero magnification it is seen that as the voltage ratios V_2/V_1 increases, the relative spherical aberration coefficient Cs/f_i decreases but the relative chromatic aberration coefficient Cc/f_i , respectively increasing linearly. At ($V_2/V_1 = 8$) the value of Cs/f_i has a minimum value equal (66.5079). When ($V_2/V_1 = 2$) the value of Cc/f_i has a minimum value equal (3.048119) (Fig. 9).

Under finite magnification condition. The spherical and chromatic aberration coefficient Cs and Cc ,

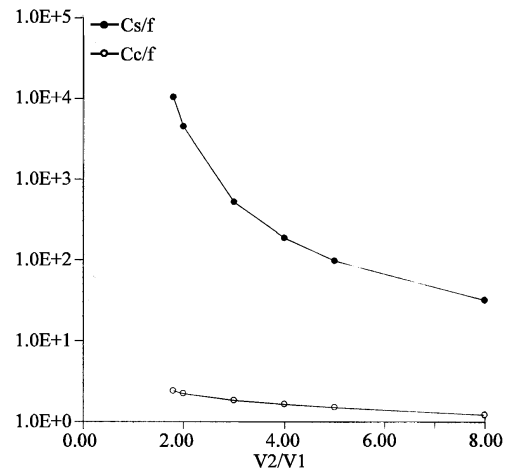


Fig. 10: The spherical and chromatic aberration coefficients under infinite magnification condition

respectively have been normalized in terms of the magnification M since in the finite mode of operation M is more important than the focal length f . It is seen that as the voltage ratios (V_2/V_1) increase, the relative spherical aberration coefficients Cs/M are decreases. At the voltage ratio ($V_2/V_1 = 8$) the spherical aberration coefficients has a minimum value equal (94.8507). While the relative chromatic aberration coefficient Cc/M are increases with increasing the voltage ratio V_2/V_1 . At the voltage ratio ($V_2/V_1 = 1.8$) the chromatic aberration coefficients has a minimum value equal (2.278434) (Fig. 9).

Under infinite magnification, it seen that as the voltage ratios (V_2/V_1) increasing, the relative spherical aberration coefficients Cs/f_0 are decreases. At the voltage

ratio ($V_2/V_1 = 1.8$) the spherical aberration coefficients has a minimum value ($C_s/f_0 = 32.1375$), also the relative chromatic aberration coefficient C_c/f_i are decreases and at the voltage ratio ($V_2/V_1 = 8$) the chromatic aberration coefficients has a minimum value ($C_c/f_0 = 1.21875$) (Fig. 10).

CONCLUSION

The implementation of the charge density method on the design of electrostatic lenses appears to be an excellent tool in the field of electron-optical design. The cylindrical immersion lens that has been designed by the above method is found to have different optical properties depending upon various geometrical parameters in addition to the mode of operation. For instance under zero magnification mode of operation this lens did not exhibit acceptable properties from the electron-optical point of view. However, in the infinite magnification mode of operation the lens performance was found to be excellent. The optical properties are highly dependent on the geometrical factors of the lens such as the radii and the lengths of the cylinders and the width of the air gap separating the two cylinders. Thus, one could now apply the charge density method on designing various types of electrostatic lenses.

REFERENCES

- Bonjour, P., 1980. Applied Charged Particle Optics, Part A, ed.A. Septier (Adv. Electron. Electron. Phys. Supplement, 13A) (Academic Press: New York and London), pp: 1-4.
- Cruise, D.R. and D.R. Cruise, 1963. A numerical method for determination of an electrostatic field about a complicated boundary. *J. Applied Phys.*, 34: 3477-3479.
- Fung, R., 1998. Trajectory calculation in an electrostatic positron beam using a reformulated extended charge density model. Ph.D. Thesis, Hong Kong University, Hong Kong.
- Grivet, P., 1972. *Electron optics*. Pergamon: Oxford and New York.
- Harting, E. and F.H. Read, 1976. *Electrostatic Lenses*. Elsevier: Oxford and New York.
- Hawkes, P.W., 1980. Some Approximate Magnetic Lens Aberration Formula *Optik*, 56: 293-320.
- Kolman, B., 1985. *Introductory linear algebra with applications*. Macmillan Publishing Company: New York.
- Mautz, J.R. and R.F. Harrington, 1972. Computation of rotationally symmetric Laplacian potentials. *Proc. IEE.*, 117: 850-885.
- Mulvey, T. and M.J. Wallington, 1973. *Electron lenses* *Rep. Prog. Phys.*, 36: 347-421. DOI: 10.1088/0034-4885/36/4/001.
- Paszowski, B., 1968. *Electron optics*. Itiffe Book: London.
- Read, F.H., A. Adams and Soto, J.R. Montiel, 1971. *Electrostatic cylinder lenses I: 2 element lenses* *J. Phys. E: Sci. Instrum.*, 4: 625-663.
- Renau, A., F.H. Read and J.N.H. Brunt, 1982. The charge density method of solving electrostatic problems with and without the inclusion of space-charge. *J. Phys. E: Sci. Instrum.*, 15: 347-354. DOI: 10.1088/0022-3735/15/3/025.
- Shirakawa, S., H. Igarashi and T. Homma, 1990. An analysis of ion beam trajectories by using boundary element method *IEEE Trans. Magn.*, 26: 555-558.
- Szilagy, M., 1988. *Electron and ion optics*. Plenum Press: New York.
- Van Hoof, H.A., 1980. A new method for numerical calculation of potentials and trajectories in system of cylindrical symmetry. *J. Phys. E: Sci. Instrum.*, 13: 1081-1089.